Improved Target Localization in Multi-Waveform Multi-Band Hybrid Multistatic Radar Networks

Murat Temiz, *Member, IEEE*, Hugh Griffiths, *Fellow, IEEE*, and Matthew Ritchie, *Senior Member, IEEE*

***Abstract*— This study proposes an algorithm to improve the target localization performance. This is implemented in a multi-waveform multi-band hybrid (passive and active) multistatic radar network scenario, that utilize broadcasting signals for radar sensing, in addition to the radar waveforms. Multi-waveform multi-band radar receivers can exploit the broadcast signals transmitted by non-cooperative transmitters, such as communication or broadcasting systems, for target sensing in addition to radar waveform. Hence, multiple measurements of the targets can be acquired and fused to improve the target detection and parameter estimation. Because of utilizing various waveforms, each transmitter-receiver (Tx-Rx) pair has a different range and velocity estimation accuracy, that is also affected by the bistatic geometry of the bistatic pairs. Taking this into account, this study proposes a target localization algorithm based on bistatic Cramér-Rao Lower Bounds (CRLBs) for multistatic multi-band radar networks. It is shown that modeling the entire network and evaluating the bistatic range CRLB of each bistatic pair in advance, and utilizing this information while estimating the target location significantly improves the localization accuracy. Moreover, the proposed algorithm also includes a target height estimation correction stage to achieve a better 3D localization accuracy.**

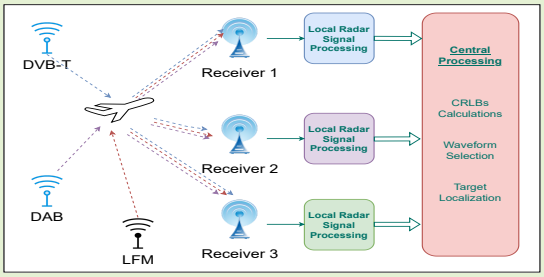

***Index Terms*— Cramér-Rao lower bounds, information fusion, multistatic radar, passive radar, radar waveform, target localization**

I. Introduction

MULTISTATIC radar networks make use of multiple distributed transmitters and receivers to perform radar sensing in the area of interest. Such radar systems have the potential to offer enhanced coverage, better target detection performance, and parameter estimation accuracy compared to single monostatic or bistatic radar systems as a result of utilizing multiple transmitters and receivers for radar sensing to acquire multiple measurements of the target at the same time [1]–[3]. However, radar transmitters are generally expensive, bulky, power-hungry, and easily detectable due to their high transmission power. For this reason, not only radar transmitters but also illuminators of opportunity (IOs), such as broadcasting and communication system signals, have been considered as radar signal sources for sensing to reduce the system cost by eliminating the need for high-power transmitters and to enable stealth sensing capabilities [4], [5]. Such radar operation is also known as passive bistatic radar as the IOs and receivers can be located at different places. As passive radar systems do not actively transmit radar waveforms, they can covertly perform target detection and estimate target parameters. Moreover, passive radar systems also contribute to spectrum management by avoiding transmitting extra radio signals in the already congested frequency spectrum. Furthermore, they are also more robust to electronic countermeasure techniques such as jamming since they make use of the signals of various broadcasting systems operating in significantly different frequency bands [1], [6], [7].

In multi-waveform passive radar systems, broadcasting signals can be acquired and processed by multi-band multi-waveform passive radar receivers for radar sensing and such receivers have been already designed, developed, and tested in [8]–[12]. Such receiver architectures were mainly designed to exploit DVB-T, DAB, and FM radio signals for radar target detection, because these broadcasting systems transmit high power and cover large areas, hence they can be utilized for long-range radar sensing applications. It is possible to create a network consisting of multiple of these receivers as a multistatic radar network, which can receive and process signals from various IOs such as FM radio, DVB-T, and DAB stations at the same time, and this will provide significant target detection and parameter estimation accuracy [13]. However, because of utilizing a wide range of signals at the same time in such radar networks, the decision of which signals to be used or fused for sensing a specific target location should be carefully evaluated.

In a hybrid multistatic radar network, target parameters acquired by all Tx-Rx pairs may be fused to improve the target detection probability or target parameter estimation accuracy

"This work was supported by the University Defence Research Collaboration (UDRC) consortium and was jointly funded by the Engineering and Physical Sciences Research Council (EPSRC) and the Defence Science and Technology Laboratory (Dstl)."

M. Temiz, H. Griffiths and M. Ritchie are with the University College London, London, WC1E 6BT, England, UK (e-mail: m.temiz@ucl.ac.uk, h.griffiths@ucl.ac.uk, m.ritchie@ucl.ac.uk).

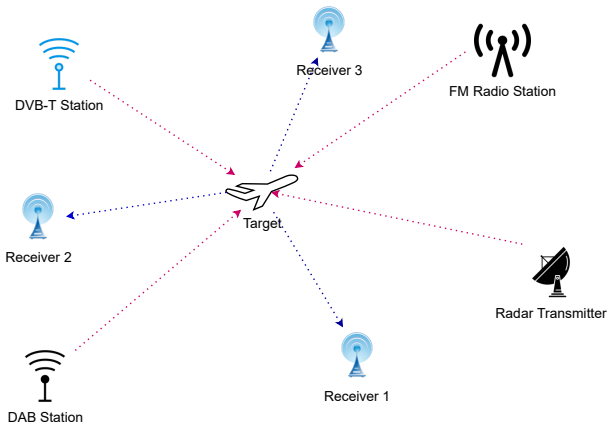

Fig. 1. A hybrid multi-waveform multi-band multistatic radar network consisting of IOs, radar transmitter and multi-band receivers.

[13], [14]. A captivating application of such fusion is estimating the two-dimensional (2D) or three-dimensional (3D) target location by utilizing the estimated bistatic range and velocity of the targets by all Tx-Rx pairs. However, the accuracies of these estimations are significantly influenced by the waveform and the bistatic geometry of the Tx-Rx pairs such that range and velocity estimation accuracies vary depending on the target location and waveforms employed for radar sensing. Since multiple waveforms, i.e., LFM, DVB-T, DAB, and FM radio signals, are utilized by receivers, a simulation model of the multistatic radar network is necessary to evaluate the estimation accuracies of Tx-Rx pairs. We previously evaluated range and velocity estimation accuracies in multi-waveform hybrid multistatic radar networks in [15], where CRLBs on the range and velocity estimations were used as performance metrics. Moreover, based on the model established in [15], the impact of the jamming in multi-waveform multistatic radar networks was also investigated [7].

Estimating the target location in radar systems can be performed by making use of various measurements of the target state such as angle of arrivals (AoA), bistatic range measurements, or time delay of the received signals. In this study, only bistatic range measurements of the target acquired by each Tx-Rx pair are considered for target localization since bistatic range measurements can be easily acquired by Tx-Rx pairs. Bistatic range measurements are estimated locally at the receivers after the range-Doppler processing on the received radar returns. Subsequently, bistatic range measurements can be conveyed to a central processing node and processed to estimate the target location. As the radar returns are locally processed at each receiver (e.g., edge computing or distributed computing) and only the estimated target parameters are conveyed to the central processing node, the amount of transmitted data and computational requirements in the central processing node are much less than the complexity of the methods that perform target localization directly from the raw data (i.e., received signals) in the central processing node, where all raw data would be transferred to the central processing node and processed there [16]. The possible locations of the target with respect to the bistatic range measurement estimated by any Tx-Rx pair form an ellipsoid of which centers are these Tx and Rx nodes. Therefore, the localization methods that utilize bistatic range measurements strive to estimate the target location by searching the target in the intersection of the ellipsoids of the bistatic range measurements estimated by all bistatic Tx-Rx pairs [17]. However, these ellipsoids may have more than one intersection, and this may lead to ghost target locations. Increasing the number of transmitters or receivers enhances the accuracy by reducing the possibility of having multiple intersection points. Tx-Rx pairs may estimate the target bistatic range with substantially different errors from each other due to the bistatic geometry, signal-to-interference-plus-noise ratio (SINR), or waveform differences and this may degrade the accuracy of the localization.

There is a large volume of published studies proposing various bistatic range-based (BR-based) target localization methods that can be employed in multistatic or distributed MIMO radar systems [18]–[30]. For instance, [27] formulates the target localization as an optimization problem and solves it in an iterative way. Although this method achieves the accuracy of an efficient estimator in most cases, it requires higher computational resources due to iteratively solving this optimization problem. Therefore, closed-form localization solutions were also proposed [21], [23], [26] to reduce the computational complexity of the target localization. Recently proposed closed-form solutions, i.e., [23], [26], [28], can more precisely estimate the target location and achieve the CRLB on the location estimation when the error covariance matrix of the bistatic estimations are known. However, localization studies have mainly assumed that the error covariance matrix of the bistatic estimations is either constant or only related to SINR of the received signals [14], [23], [26]. This assumption results in substantial errors in multi-band multi-waveform hybrid multistatic networks, where the bistatic range estimation errors and their variance rapidly vary depending on multiple factors such as the target location, bistatic geometry, SINR, and the waveforms utilized by each Tx-Rx pair. Estimating the target location based on the bistatic measurements acquired using different waveforms transmitted by IOs is therefore challenging due to the fact that each bistatic Tx-Rx pair will estimate the target bistatic range with a significantly different amount of error depending on the waveform, Tx, Rx, and target location. Moreover, as the target moves, the error in the bistatic range estimated by the same pair will also vary due to the changing bistatic geometry concerning the target location. Therefore, these methods may not perform well as expected in a hybrid multistatic radar network due to the waveform diversity of pairs and the impact of the geometry that continuously varies as the target moves. As a consequence, we propose an algorithm that utilizes the CRLBs on bistatic range estimations of the pairs to improve the accuracy of target localization in hybrid multistatic radar networks. Accordingly, the main motivation of this study is to investigate the target localization problem in multi-band multi-waveform hybrid multistatic networks and to propose a method to improve its accuracy. The proposed method also consists of a technique to correct the target height estimation that is more challenging due to the limited diversity in the height of transmitters, IOs,

and receivers. The proposed technique has been shown to improve the overall localization accuracy and it can more efficiently utilize the IOs that have high estimation errors due to the limited bandwidth.

Consequently, we have created a framework to model the hybrid multistatic radar networks and calculate the CRLBs on range and velocity of the targets. Then, by utilizing CRLBs on the range estimations, we have proposed a target location estimation algorithm that more efficiently utilizes broadcasting signals in addition to radar signals for target localization. Although any localization method can be used within the proposed technique in this study, we have chosen the localization method recently proposed in [23], because this method can approximately reach the CRLBs of the target location estimation and it can work with fewer number of Tx-Rx pairs compared to other methods. Moreover, a further step has been proposed to improve the accuracy of the target height estimation in 3D scenarios, which is a necessary step as the diversity in the heights of transmitters and receivers is limited. Although this study mainly focuses on radar networks as an example, the proposed method can also be used in other type of sensor networks to improve the location estimation.

The contributions of this research are:

- It models the multi-waveform multi-band hybrid multistatic radar networks to investigate the accuracy of bistatic range measurements and target localization accuracy that are achieved under various scenarios.
- It proposes a 3-stage algorithm by utilizing CRLBs on the range to improve the target localization accuracy in hybrid multistatic radar networks, where the accuracy of bistatic range measurements are highly dependent on the waveform and the bistatic geometry.
- It also proposes a method to refine the target height estimation using CRLBs on the range to further improve the 3D target localization performance.

In the rest of this paper, Section II introduces the system model while Section III explains the bistatic range estimations, target location estimation and the proposed algorithm. Section IV presents the numerical results and evaluates the proposed algorithm. Finally, the conclusions are drawn in Section V.

II. System Model

The multistatic radar network model considered in this research consists of an active radar transmitter, multiple IOs and multi-band multi-waveform radar receivers that locally process the signals reflected from the targets for radar sensing and convey the estimated range and velocity information to a central processing node. DVB-T, DAB and FM radio stations are considered as IOs of which non-cooperative signals are exploited by multi-band multi-waveform radar receivers for passive radar sensing. Therefore, multiple bistatic measurements of the target can be acquired at the receivers. [1]

Fig. 1 illustrates an example hybrid multistatic radar network consisting of a transmitter, IOs and multi-band receivers.

[1]The active radar transmitter and IOs and receivers are assumed to be placed at different locations, therefore, only bistatic radar measurements are acquired and considered for target localization. Thus, monostatic radar measurements are not considered for target localization in this study.

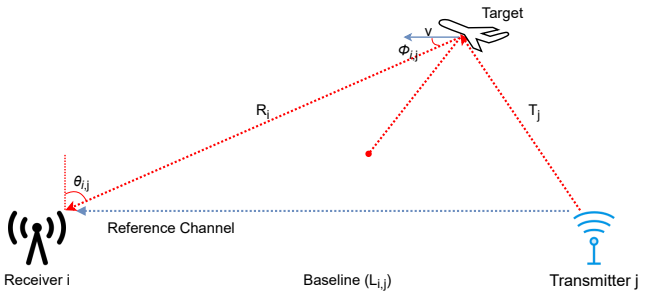

Fig. 2. Illustration of the bistatic geometry between the transmitter, target and receiver.

As the transmitters and receivers can be placed at different locations, a bistatic geometry between each transmitter, the target and each receiver can be observed as shown in Fig. 2. The bistatic geometry affects the bistatic target radar cross-section (RCS), target detection and bistatic range, and velocity estimations especially when the target approaches the baseline of the Tx-Rx pair [4], [31]. This study utilizes the CRLB on the range, which is a function of bistatic geometry, SINR, and waveform, to improve the target localization accuracy in the multistatic active/passive radar network. Therefore, the bistatic CRLB expressions, considered waveforms, and their parameters will also be reviewed in the following sections.

A. Multi-waveform multi-band receivers

The multi-band radar receivers exploit the signals transmitted by the radar transmitter and broadcasting stations (IOs) for radar sensing. They also need to acquire the reference signals directly from the IOs to compare with the reflected signals from the targets for radar sensing. Multi-band radar receivers employ multiple antennas and radio frequency (RF) channels in order to utilize multiple IOs at the same time. For example, different prototypes of such multi-band multi-waveform receivers were designed, implemented, also tested in [5], [8], [9] and these studies demonstrated that DVB-T, DAB, and FM radio signals can be effectively and jointly utilized for passive radar sensing. Moreover, by deploying multiple multi-waveform multi-band receivers and coordinating them through a central processing unit, it is possible to create an intelligent hybrid multistatic radar network as considered in this study.

B. Radar Waveform and Broadcasting Signals

For active radar sensing, an X-band (10 GHz) radar transmitter is considered, which transmits LFM pulse bursts. Moreover, DVB-T, DAB, and FM radio stations are considered as IOs, which transmit broadcasting signals in their allocated frequency bands. Since the frequency bands of all considered waveforms are well separated, they do not have any interference between them. DVB-T and DAB systems employ orthogonal frequency division multiplexing (OFDM) signals while FM radio stations transmit frequency modulated (FM) signals with a narrower bandwidth and a lower carrier frequency compared to the other mentioned broadcasting systems. The bandwidth of FM waveforms is around 100 kHz and this results in a coarse range resolution, however, FM

radio-based passive radar can achieve a better target range estimation accuracy than its range resolution as demonstrated by measurements in [17]. For instance, the standard deviation of bistatic range measurements using FM radio signals was shown to be 120-567 m in [17]. Our previous study on bistatic CRLBs and multistatic radar networks also presented that 180-1500 m bistatic range estimation accuracy can be achieved via FM radio signals depending on the SINR and the bistatic geometry [15].

C. Radar Channel Model

The multistatic radar model consists of I multi-band multi-waveform receivers that receive signals from J transmitters or IOs available in the area of interest. Receivers are assumed to be synchronized with the active radar transmitter while they also employ reference antennas to acquire the reference signals from IOs and utilize surveillance antennas so that they can also collect and process the reflected signals from the target from the transmitted signals by the IOs. Fig. 2 illustrate the bistatic geometry between the jth transmitter and the ith receiver, where the bistatic baseline is denoted by $L_{i,j}$. Moreover, the distance between the target and the jth transmitter is denoted by T_j and the distance between the target and the ith receiver is denoted by R_i. θ_i denotes the angle between the receiver and the target while $\phi_{i,j}$ denotes the angle of the target velocity vector to the bistatic bisector. Accordingly, the relative velocity of the target is given by $V_{i,j} = V \cos \phi_{i,j}$, where V denotes the velocity of the target. IOs, targets and receivers are located at (x_j, y_j, z_j), (x_t, y_t, z_t), (x_i, y_i, z_i) points, respectively in a 3D coordinate system. Moreover, B_j and f_j denote the bandwidth and the carrier frequency of the waveform transmitted by the jth transmitter.

The received signal at the surveillance antenna of the ith receiver from the jth transmitter (or IO) after reflecting from a single target is given by

$$x_{ij}(t) = \sqrt{\xi_{i,j}(t)} u_j(t-\tau_r) + \sqrt{\alpha_{i,j}(t)\,\sigma_t} u_j(t-\tau) e^{-j2\pi\omega(t)} + n_i(t), \quad (1)$$

where $u_j(t)$ is the transmitted signal by the jth transmitter (LFM, DVB-T, DAB or FM radio signals), $\alpha_{ij}(t)$ denotes the channel gain that consists of transmit power, transmitter and receiver antenna gains and path loss, σ_t denotes the RCS of the target, and $n_i(t) \sim \mathcal{CN}\left(0, \sigma_i^2\right)$ is the AWGN noise at the surveillance channel of the ith receiver. The delay caused by the target range and the Doppler frequency caused by the target velocity are denoted by τ and ω, respectively. Moreover, the delay in the reference channel is denoted by τ_r, and the direct-path interference (DPI) is denoted by $\xi_{i,j}(t)\, u_j(t-\tau_r)$ where $\xi_{i,j}$ is the product of the transmit power, antenna gain and path loss of the direct path between the jth transmit antenna and the ith surveillance receive antenna. The transmitters and IOs operate at different carrier frequencies, therefore, any interference between them is not considered.

The reference signal acquired by a reference antenna is given by

$$y_{i,j}(t) = \sqrt{\psi_{i,j}(t)} u_j(t-\tau_r) + n_{r,i}(t), \quad (2)$$

where $\psi_{i,j}$ is the product of the transmit power, antenna gain and path loss between the jth IO and the ith receiver's reference antenna and $n_{r,i}(t)$ is the noise at the reference channel of the ith receiver. The reference antenna is typically directed to the IO to maximize the SINR of the reference signal, hence, $\psi_{i,j} > \xi_{i,j}$. Further to this, the surveillance and reference antenna channels have the same bandwidth, hence $n_{r,i}(t) = n_i(t)$. If the SINR of the reference channel is sufficient, the noise in the reference channel can be neglected, however, in low SINR cases, it affects the passive radar sensing [32]. Accordingly, considering both the noises in the reference and surveillance channels, SINR of the received signal is modeled by

$$\rho_{i,j} = \frac{\alpha_{i,j}(t)\,\sigma_t}{2\sigma_i^2 + \mu_{DPI}\xi_{i,j}(t)}, \quad (3)$$

where $0 \leq \mu_{DPI} \leq 1$ denotes the residual direct-path interference (DPI) ratio after DPI cancellation as passive radar systems utilize DPI cancellation algorithms such as filters or multistage disturbance cancellation algorithms [33], [34]. For the active bistatic radar case, SINR is given by $\rho_{i,j} = \frac{\alpha_{i,j}(t)\sigma_t}{\sigma_i^2}$ as the waveform transmitted by the radar transmitter is known by the receiver and synchronized, hence the active radar operation does not require a reference antenna. Parameters $\alpha_{i,j}$, $\psi_{i,j}$ and $\xi_{i,j}$ are calculated using the radar and path-loss equations as in [33]. The noise variance at the ith receiver is modeled as $\sigma_i^2 = k_B T_0 B_i N_F$, where k_B, B_i, T_0 and N_F denote the Boltzmann's constant (1.38×10^{-23} J/K), the bandwidth of the ith receiver, temperature (290 K) and receiver noise figure.

D. Bistatic CRLBs on Range and Velocity Estimations

The CRLB determines the theoretical lower bound on the variance of estimations that an efficient unbiased estimator can achieve while estimating deterministic unknown parameters. Target velocity and range estimation errors in radar systems are also lower bounded by CRLBs such that the variance of the estimation errors can be equal to or higher than the CRLBs. Therefore, CRLBs are widely used as a performance benchmark to evaluate the performance of estimation techniques and algorithms. It was shown that monostatic CRLBs on range and velocity estimations can be derived from ambiguity functions of the radar waveform [35]. Furthermore, for the bistatic radar, the bistatic CRLBs can be written as a function of bistatic geometry and monostatic CRLBs [31].

The estimated bistatic ranges by the bistatic pairs are related to the waveform, bistatic geometry and SINR, therefore, it varies as the target moves. The bistatic CRLBs on the range and velocity estimations performed using the jth transmitter and the ith receiver are respectively given by

$$CRLB(R_{i,j}) = \frac{\mathbf{J}(R_{i,j}, V_{i,j})_{2,2}}{\det\left[\mathbf{J}(R_{i,j}, V_{i,j})\right]}, \quad (4)$$

$$CRLB(V_{i,j}) = \frac{\mathbf{J}(R_{i,j}, V_{i,j})_{1,1}}{\det\left[\mathbf{J}(R_{i,j}, V_{i,j})\right]}, \quad (5)$$

where $\mathbf{J}(R_{i,j}, V_{i,j})_{2,2}$ and $\mathbf{J}(R_{i,j}, V_{i,j})_{1,1}$ denote the $(2,2)$th and $(1,1)$th elements of the bistatic Fisher Information Matrix

(FIM) $\mathbf{J}(R_{i,j}, V_{i,j})$ between the jth transmitter and the ith receiver, respectively. The bistatic FIM for range and velocity estimations performed by the jth transmitter and the ith receiver pair is defined by

$$\mathbf{J}(R_{i,j}, V_{i,j}) = -2\rho_{i,j} \begin{bmatrix} \frac{\partial^2 \Theta(R_{i,j}, V_{i,j})}{\partial R_{i,j}^2} & \frac{\partial^2 \Theta(R_{i,j}, V_{i,j})}{\partial R_{i,j} \partial V_{i,j}} \\ \frac{\partial^2 \Theta(R_{i,j}, V_{i,j})}{\partial V_{i,j} \partial R_{i,j}} & \frac{\partial^2 \Theta(R_{i,j}, V_{i,j})}{\partial V_{i,j}^2} \end{bmatrix}, \quad (6)$$

where $R_{i,j}$ denotes the bistatic range of the target for the ith transmitter and jth receiver and $\rho_{i,j}$ denotes the SINR of the radar returns, which is given by (3). The partial derivatives in (6) are calculated as [31],

$$\frac{\partial^2 \Theta\left(R_{i,j}, V_{i,j}\right)}{\partial R_{i,j}^2} = \left[\mathbf{J}_0\right]_{1,1} \left(\frac{\partial \tau}{\partial R_{i,j}}\right)^2 + 2\left[\mathbf{J}_0\right]_{1,2} \frac{\partial \tau}{\partial R_{i,j}} \frac{\partial \omega}{\partial R_{i,j}} + \left[\mathbf{J}_0\right]_{2,2} \left(\frac{\partial \omega}{\partial R_{i,j}}\right)^2, \quad (7)$$

$$\frac{\partial^2 \Theta\left(R_{i,j}, V_{i,j}\right)}{\partial V_{i,j}^2} = \left[\mathbf{J}_0\right]_{2,2} \left(\frac{\partial \omega}{\partial V_{i,j}}\right)^2, \quad (8)$$

$$\frac{\partial^2 \Theta\left(R_{i,j}, V_{i,j}\right)}{\partial R_{i,j} \partial V_{i,j}} = \left[\mathbf{J}_0\right]_{1,2} \frac{\partial \tau}{\partial R_{i,j}} \frac{\partial \omega}{\partial V_{i,j}} + \left[\mathbf{J}_0\right]_{2,2} \frac{\partial \omega}{\partial R_{i,j}} \frac{\partial \omega}{\partial V_{i,j}}. \quad (9)$$

In these derivations, $R_{i,j}$ and $V_{i,j}$ denote the bistatic range and velocity while τ and ω denote the delay and the Doppler frequency, respectively. $\mathbf{J}_0$ denotes the waveform-related part of the FIM, which is only a function of the waveform itself and it is given by

$$\mathbf{J}_0 = \begin{bmatrix} \frac{\partial^2 \Theta(\tau,\omega)}{\partial \tau^2} & \frac{\partial^2 \Theta(\tau,\omega)}{\partial \tau \partial \omega} \\ \frac{\partial^2 \Theta(\tau,\omega)}{\partial \omega \partial \tau} & \frac{\partial^2 \Theta(\tau,\omega)}{\partial \omega^2} \end{bmatrix}. \quad (10)$$

Equations between (7) and (10) show that the bistatic CRLBs on the range and velocity estimations can be decoupled into only waveform and only bistatic geometry and SINR dependent parameters. As a consequence, both the bistatic geometry and waveform parameters significantly impact the CRLBs, hence range and velocity estimation accuracies. Closed-form equations of geometry-related FIM derivatives were given in [15], [31], therefore they are not given here for the sake of brevity. Waveform related parts of the FIM were derived and given for LFM waveform in [35], OFDM signals in [36] and FM radio signals in [37]. It is worth noting that the FIMs for OFDM and FM signals were derived based on averaged signals since these broadcasting signals vary over time depending on the content transmitted [36], [37]. DVB-T and DAB signals are fundamentally OFDM signals with different modulation parameters such as subcarrier spacing and waveform duration. Accordingly, the FIM of the OFDM signals is used with DVB-T and DAB signal parameters to model their FIMs.

E. LFM Radar Waveform

The closed-form FIM for a burst waveform consisting of N LFM pulses is given by [31], [35],

$$\mathbf{J}_{LFM} = \begin{bmatrix} \frac{-k^2\pi^2 T_p^2}{3} & \frac{k\pi^2 T_p^2}{3} \\ \frac{k\pi^2 T_p^2}{3} & \frac{\pi^2 T_R^2\left(1-N^2\right)-\pi^2 T_p^2}{3} \end{bmatrix}, \quad (11)$$

where T_p, T_R and N denote the duration of each pulse, pulse repetition interval and number of LFM pulses transmitted. Moreover, k is defined as $k = B/T_p$, the ratio of the LFM pulse bandwidth, $B = f_1 - f_0$, to the pulse duration T_p. The details of these closed-form expressions can be found in [31], [35].

F. OFDM Signals

DVB-T and DAB broadcasting systems both transmit OFDM signals, however with different OFDM parameters. Nevertheless, the same modified FIM derivations can be applied to calculate CRLBs of these signals. The modified (averaged) FIM is used for the calculation of CRLBs of OFDM signals since they also vary over time depending on the data transmitted in its subcarriers. The elements of the FIM for OFDM signals consisting of L symbols over N_s subcarriers are given by [15], [36],

$$\left[\mathbf{J}_{OFDM}\right]_{1,1} = \frac{4\pi^2 L\left(3+\Delta f^2\left(N_s^2-1\right)\left(4T_{sym}-T_w\right)T_w\right)}{\left(48T_{sym}-12T_w\right)T_w}, \quad (12)$$

$$\left[\mathbf{J}_{OFDM}\right]_{2,2} = \frac{L}{12T_{sym}-3T_w/4}[4\pi^2 L^2 T_{sym}^3 - \pi^2\left(L^2+2\right)T_{sym}^2 T_w - \left(\pi^2-6\right)T_w^3 + 12\left(\pi^2-8\right)T_{sym}T_w^2], \quad (13)$$

and $\left[\mathbf{J}_{OFDM}\right]_{1,2} = \left[\mathbf{J}_{OFDM}\right]_{2,1} = 0$, where Δf, T_{sym}, T_{cp}, T_w denote the OFDM subcarrier spacing, symbol duration, cyclic-prefix duration and windowing duration of the OFDM symbols, respectively [36].

G. FM Radio Signals

FM radio signals have been widely considered for passive radar operations [17] and their modified FIM expressions were derived as [37],

$$\mathbf{J}_{SFM} = \begin{bmatrix} 4\pi^2\beta^2 f_0^2 & -(-1)^z 2\pi\beta\sin(\phi) \\ -(-1)^z 2\pi\beta\sin(\phi) & \frac{\pi^2 T_{FM}^2}{3} \end{bmatrix}, \quad (14)$$

where the approximate bandwidth of FM signal is given by Carson's bandwidth as $B_{FM} = 2(\delta f + f_m) = 2\beta f_0$, where δf and f_m denote the peak frequency deviation and the highest frequency in the modulated signal. Moreover, ϕ and T_{FM} denote the phase and observation time of FM signals for passive sensing.

III. Bistatic Range and Location Estimations

The aforementioned BR-based target location estimation methods [18]–[29] require the variance of the bistatic ranges estimated by Tx-Rx pairs to achieve an accurate target location estimation since the target localization is significantly affected by the bistatic range estimation errors. However, it is difficult to directly know the variance of the bistatic range estimations since it varies depending on the target location as well as the waveform parameters. Accordingly, we exploit the relation between the CRLBs on the range and variance of the range estimation in this study. The bistatic range estimation errors are lower-bounded by the bistatic CRLB on the range of the corresponding Tx-Rx pair. Accordingly, bistatic CRLBs on the range of the pairs are utilized to take into account the bistatic range estimation errors while estimating the target location in this study.

The bistatic CRLB on the range varies depending on the target location and waveform of the bistatic pairs, therefore, the range estimation error of each pair will be different for different target locations. However, calculating the CRLB of all pairs for the entire area of interest will reveal the expected average range estimation errors for different pairs. Based on the CRLBs map of the area, the range information acquired by Tx-Rx pairs are fused for target localization. As the location of the target is unknown, firstly the average CRLBs of the pairs are used for the initial target location estimation. Afterward, the second estimation is performed based on the coarsely estimated initial target location and corresponding CRLB on range to this location.

A. Target Location Estimation

Let $\hat{R}_{i,j,k}$ denote the estimated bistatic range by the ith transmitter and jth receiver for the kth target location as

$$\hat{R}_{i,j,k} = R_{i,j,k} + \xi_{i,j,k}, \tag{15}$$

where $R_{i,j,k}$ denotes the true bistatic range of the kth target location to the (i,j)th Tx-Rx pair, and $\xi_{i,j,k}$ denotes the estimation error, which is assumed to follow a Gaussian distribution with zero mean and variance $\sigma^2_{i,j,k}$ as $\xi_{i,j,k} \sim \mathcal{N}(0, \sigma^2_{i,j,k})$. The variance of this range estimation is lower bounded by the CRLB on the range of the (i,j)th Tx-Rx pair for the kth location as

$$\sigma^2_{i,j,k} \geq CRLB(R_{i,j,k}), \tag{16}$$

where $CRLB(R_{i,j,k})$ denote the CRLB on the range estimations of the $(i.j)$th Tx-Rx pair for the kth target location. The CRLB information matrix of the entire area of interest is computed in advance using (7)-(10), therefore, it is known by the radar system.

The true bistatic range of the kth target to the $(i.j)$th Tx-Rx pair is calculated as

$$\begin{aligned} R_{i,j,k} &= R_{i,k} + R_{k,j} \\ &= \sqrt{(x_i - x_k)^2 + (y_i - y_k)^2 + (z_i - z_k)^2} \\ &+ \sqrt{(x_j - x_k)^2 + (y_j - y_k)^2 + (z_j - z_k)^2}, \end{aligned} \tag{17}$$

where x, y and z with subscripts i, j and k denote the coordinates of the ith receiver, jth transmitter and kth target, respectively. The locations of the transmitters and receivers are known, therefore, the 3D location of the target, denoted by $[x_k, y_k, z_k]$, can be estimated using multiple bistatic range measurements $\hat{R}_{i,j,k}$ acquired by multiple bistatic pairs (e.g., 2 transmitters and 2 receivers) [23]. The target location estimation can be formulated as a maximum likelihood estimation problem as

$$\underset{[\tilde{x}_k, \tilde{y}_k, \tilde{z}_k]}{\arg\min} \sum_{i=1,j=1}^{I,J} \left| \hat{R}_{i,j,k} - \tilde{R}_{i,j,k} \right|^2, \tag{18}$$

where $\hat{R}_{i,j,k}$ was given by (15) and

$$\begin{aligned} \tilde{R}_{i,j,k} &= \sqrt{(x_i - \tilde{x}_k)^2 + (y_i - \tilde{y}_k)^2 + (z_i - \tilde{z}_k)^2} \\ &+ \sqrt{(x_j - \tilde{x}_k)^2 + (y_j - \tilde{y}_k)^2 + (z_j - \tilde{z}_k)^2}, \end{aligned} \tag{19}$$

and $[\tilde{x}_k, \tilde{y}_k, \tilde{z}_k]$ denotes the estimated target location.

The maximum likelihood estimation problem given by (18) can be solved by optimization problem solvers, however, it is non-convex and does not take the estimation errors into account. Therefore, the solvers may not reach the global solution. Accordingly, several single-stage or multiple-stage target location estimation techniques and closed-form equations have been proposed [18]–[30]. In this study, any of these estimation methods can be employed since we propose a framework which combines target localization methods and bistatic CRLB on the range information of the pairs to improve the estimation performance. As the localization method recently proposed in [23] outperforms other methods with reasonable computational complexity, we employed this efficient localization method as an example in our algorithm in this study. The method in [23] is a closed-form two-staged weighted least squares localization method, therefore its computational complexity is low and it can be efficiently executed within the proposed algorithm. The proposed algorithm consists of four stages. The first stage is to calculate the CRLB on the range of the area and create a lookup table that consists of the CRLB on the range information corresponding to all possible target locations. This is calculated with 1×1 km^2 resolution for all pairs, i.e. CRLB on the range of each pair is calculated for each 1×1 km^2 area. 1×1 km^2 resolution is chosen for the CRLBs on range calculations, because, our previous study [15] has shown that this resolution provides a good accuracy in terms of CRLBs calculations of the entire area for FM radio, DAB and DVB-T signals. The size of the precalculated CRLB lookup table matrix is $X \times Y \times I \times J$ consisting of all CRLB on the range information for $X \times Y$ km^2 area observed by I receivers and J IOs. It is worth noting that example CRLB on range figures of the entire area of interest were given in [15], therefore, we would like to refer the interested readers to [15] for more details of this calculation for the sake of brevity. As the target location is initially unknown, the averaged CRLB on range of each pair for the entire area of interest is calculated and used in the initial target location estimation. To calculate the averaged CRLB on range of each pair, let $K = X \times Y$ denote the number of possible target locations for $X \times Y$ km^2 area,

the average CRLB on the range for the ith receiver and the jth IO pair can be calculated as

$$CRLB(R_{i,j}) = \frac{1}{K}\sum_{k=1}^{K}\left[CRLB(R_{i,j,k})\right], \tag{20}$$

where $k = 1, 2, \ldots, K$ denotes the target location at (X_k, Y_k) coordinates. The initial error covariance matrix of the bistatic range estimations is calculated using the average CRLBs on the range of all Tx-Rx pairs as

$$\mathbf{Q}_e = \begin{bmatrix} CRLB(R_{1,1}) & 0 & 0 & 0 \\ 0 & CRLB(R_{1,2}) & 0 & 0 \\ 0 & 0 & ... & 0 \\ 0 & 0 & 0 & CRLB(R_{I,J}) \end{bmatrix}, \tag{21}$$

for I receivers and J transmitters. Covariance matrix (21) is used in the closed-form localization method given by [23] to estimate the initial target location based on the bistatic range measurements. In the next stage, the corresponding CRLBs on the range for all pairs of the initially estimated target location are fetched from the CRLB lookup table of the entire area. Therefore, in the second stage, the elements of the covariance matrix $\mathbf{Q}_e$ given by (21) will be updated with the CRLBs on the range of initially estimated target location $\tilde{k}$ for all Tx-Rx pairs as

$$CRLB(R_{i,j}) \leftarrow CRLB(R_{i,j,k}) : k = \tilde{k}. \tag{22}$$

Subsequently, the closed-form localization method is performed again using the estimated bistatic ranges and the new covariance matrix. In the last stage, the target height estimation is improved by using the estimated x and y coordinates and bistatic CRLBs on the range of all pairs.

B. Target Height Estimation Correction

The localization methods reported in the literature are generally able to estimate the target position with reasonable error in the x and y coordinates, however they tend to produce a larger error in the z coordinate (target height) estimation. This is due to the highest positioned node out of all the transmitters' and receivers' included within the scene being at a much lower altitude than the target height. For this problem, we propose another stage in the algorithm, which aims to revise the height estimation via utilizing the estimated x and y coordinates of the target, estimated bistatic ranges, and CRLBs on the range of the Tx-Rx pairs. The target height correction stage is formulated as an optimization problem to minimize the 3D target location estimation error calculated based on the estimated bistatic ranges and previously estimated target x and y positions in order to find the enhanced target height estimation, $\tilde{z}_k$, as

$$\underset{\tilde{z}_k}{\arg\min} \sum_{i=1,j=1}^{I,J} \left| \frac{\hat{R}_{i,j,\tilde{k}} - \tilde{R}_{i,j,\tilde{k}}}{CRLB(R_{i,j,\tilde{k}})} \right|^2, \tag{23}$$

and $z_{min} \leq \tilde{z}_k \leq z_{max}$, where z_{min} and z_{max} denote the minimum and maximum possible target heights. Optimization problem (23) can be easily solved by any optimization solver or by searching the optimum $\hat{z}_k$ since it is a single variable optimization problem.

C. Target Location Estimation Accuracy Performance

As a performance metric, the mean absolute estimation error (MAE) of the target location is considered. For N target location estimations, the MAE of x-position estimations of the target is calculated as

$$\xi_x = \frac{1}{N}\sum_{n=1}^{N} |\tilde{x}_n - x_n|, \tag{24}$$

where x_n and $\tilde{x}_n$ denote the target's x-position and its estimation in the nth estimation. This can be also applied for y- and z-position estimations to calculate ξ_y and ξ_z. Consequently, the overall MAE of the estimations, ξ_o is calculated by $\xi_o = \frac{1}{3}(\xi_x + \xi_y + \xi_z)$.

The proposed method for target localization based on BR measurements is summarized in Algorithm 1, where the size of the area of interest is defined by $X \times Y$ in x and y coordinates. The resolution of the CRLB calculations is ΔX and ΔY while calculating the CRLBs on the range of the entire area of interest in advance. This three-stage algorithm is computationally efficient since it is based on closed-form equations and the target height correction stage is a single variable optimization problem. The generated CRLBs table for the entire area of interest can be saved and reused again as long as the locations of the transmitters and receivers are kept constant.

Algorithm 1: Target Localization Estimation by Utilizing CRLBs on Range

Input: $\mathbf{x}_i, \mathbf{x}_j, R_{i,j} \forall (i,j,k) \in (I,J,K)$
Output: $[\tilde{x}_k, \tilde{y}_k, \tilde{z}_k]$
Calculate mean CRLB on range for each Tx-Rx pair;
while $X_t \leq X$ **do**
  while $Y_t \leq Y$ **do**
    $k \leftarrow (X_t, Y_t)$
    Calculate $CRLB(R_{i,j,k})$ for all pairs via (4);
    $Y_{t+1} \leftarrow Y_t + \Delta Y$
  end
  $X_{t+1} \leftarrow X_t + \Delta X$
end
First Stage $CRLB(R_{i,j}) = \frac{1}{k}\sum_k [CRLB(R_{i,j,k})]$
Estimate Initial Target Location $[\tilde{x}_k, \tilde{y}_k, \tilde{z}_k]$;
while *Bistatic Range Estimations* **do**
  Estimate the initial target position using the method in [23] with $\mathbf{Q}_e$ given by (21);
end
Second Stage ;
Update the $\mathbf{Q}_e$ using the initially estimated target location $[\tilde{x}_k, \tilde{y}_k, \tilde{z}_k]$ as ;
$CRLB(R_{i,j}) \leftarrow CRLB(R_{i,j,k}) : k = \tilde{k}$;
while *Bistatic Range Estimations* **do**
  Re-estimate the target position using the updated $\mathbf{Q}_e$;
end
Third Stage ;
Re-estimate the target height via (23)
Return the final estimated target location $[\tilde{x}_k, \tilde{y}_k, \tilde{z}_k]$

TABLE I
THE LOCATIONS OF TRANSMITTERS AND RECEIVERS IN THE EXAMPLE SCENARIO AND TRANSMITTED WAVEFORMS BY IOS.

ID	Waveform	x-position	y-position	z-position [Height]
Tx1	LFM Waveform	1000 m	1500 m	3 m
Tx2	DVB-T Signals	18000 m	18000 m	12 m
Tx3	DAB Signals	8000 m	4000 m	14 m
Tx4	FM radio Signals	20000 m	5000 m	10 m
Rx1	Multi-band Receiver	1500 m	2000 m	3 m
Rx2	Multi-band Receiver	8000 m	13000 m	2 m
Rx3	Multi-band Receiver	5000 m	6000 m	4 m
Rx4	Multi-band Receiver	18000 m	1000 m	2 m

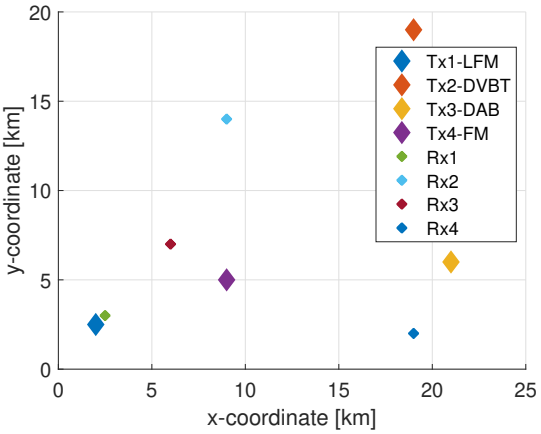

Fig. 3. An example scenario consisting of the radar transmitter, IOs and receivers in the area of interest.

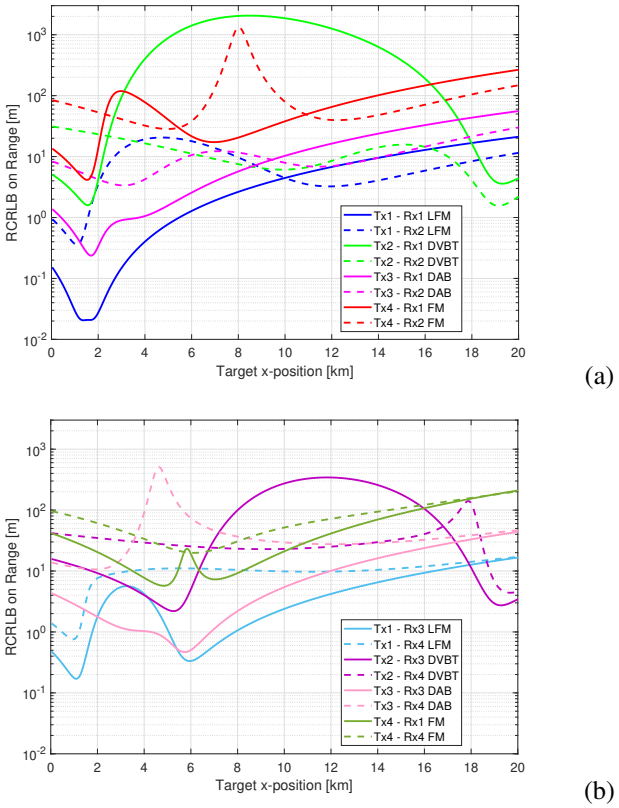

Fig. 4. CRLBs on the range for a) Rx1 and b) Rx2 receivers with all transmitters and IOs while the target moves in the example scenario.

IV. NUMERICAL RESULTS

In the simulations, one radar transmitter (LFM waveform) and three IOs (DVB-T, DAB and FM radio), and four multi-waveform multi-band receivers are considered for multistatic radar sensing and target localization. An example scenario is given in Fig. 3, where the locations of the transmitter, IOs, and receivers are shown and more details about them are given in Table I. It can be seen that the maximum height of the receivers is 4 m, and the maximum height of transmitters is 15 m, this does not provide sufficient diversity for a precise target height estimation since the target height can be up to a few km. The target is assumed to follow a sinusoidal trajectory in terms of altitude, as shown in Fig.11, to challenge the proposed method in the simulations. The numerical results presented in this section are obtained by averaging many scenarios consisting of randomly located IOs, receivers and 10 different target trajectories to provide more generic results and comparisons, i.e., independent of the scenarios, between the methods proposed in this study.

The waveforms transmitted by the radar transmitter and IOs and their parameters considered in the simulations are given in Table II, where LFM signals are transmitted by the radar transmitter and the DVB-T, DAB, and FM radio signals are transmitted by IOs. The radar transmitter operates at 10 GHz frequency with 50 MHz bandwidth and utilizes high gain transmit and receive antennas. Therefore, the LFM waveform is expected to outperform other waveforms for target range

TABLE II
RADAR WAVEFORM AND IO SIGNALS

Waveform	Parameters	Antenna
LFM waveform	f_c = 10 GHz B = 50 MHz N = 64 P_t = 5 KW T_p = 200 μs T_R = 400 μs	Directive (10 dBi)
DVB-T signals (OFDM Waveform)	f_c = 500 MHz Δ_f = 1116 kHz N_s = 6817 B = 7.61 MHz L = 64 T_{sym} = 896 μs $T_w = T_Q/4$ P_t = 5 KW	Omnidirectional
DAB Signals (OFDM Waveform)	f_c = 200 MHz Δ_f = 2000 kHz N_s = 768 B = 1.54 MHz L = 64 T_{sym} = 623 μs $T_w = T_Q/4$ P_t = 5 KW	Omnidirectional
FM Radio	f_c = 100 MHz f_0 = 15 kHz β = 5 B_{FM} = 75 kHz T_{FM} = 100 ms P_t = 15 KW ϕ = 0	Omnidirectional

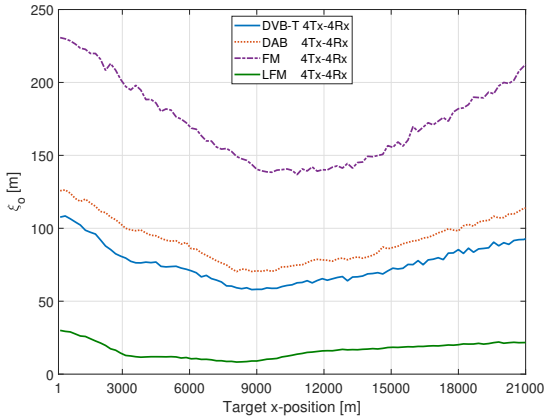

Fig. 5. Mean localization errors if all 4 transmitters transmit the same type of waveforms (e.g., 4 DVB-T transmitters) in the example scenario shown in Fig. 3.

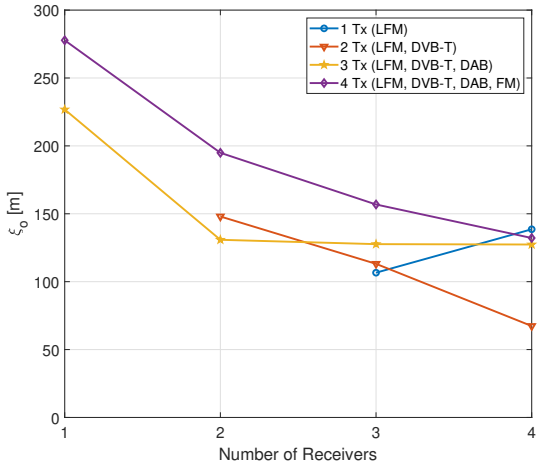

Fig. 6. Average target localization error of the multistatic network with various number of Tx and Rx combinations without CRLB on range information of the Tx-Rx pairs.

estimation, however other waveform options might provide a better range estimation accuracy due to the impact of the geometry in some target locations. Table II also shows that the radar transmitter and broadcasting systems operate in significantly different frequency bands from each other, and this provides a frequency diversity in the multistatic radar operation, resulting in interference and jamming robust radar system.

The impact of the geometry and waveform on the range estimations are presented in an example scenario in Fig. 4, where root CRLBs (RCRLB, i.e., $\sqrt{CRLB}$) on the range estimations of all pairs are illustrated for the multistatic radar scenario given in Fig. 3. Fig. 4 (a) illustrates the CRLBs with Rx1 and Rx2 and Fig. 4 (b) CRLBs with Rx3 and Rx4. These figures clearly show that LFM waveform provides the overall best range estimation accuracy however other waveforms may provide better range estimations in some specific target locations where the active radar (LFM waveform) pairs encounter forward scatter problem as the target approaches the baseline, or the SINR of the active radar pairs may not be sufficient to detect and estimate the target parameters. CRLBs results are calculated for the entire area of interest, 20×20 km^2 area, with 1 km^2 resolution. This turns out 400 CRLB on range estimation for each Tx-Rx pair. Since 4 Tx and 4 Rx are considered, the total number of Tx-Rx pairs is 16. Since initially the radar system does not have any information regarding the target location, it utilizes the mean of the CRLBs for each pair for the initial estimation as explained.

Fig. 5 compares the target location estimation accuracy of 4 different waveform types (i.e., LFM, DVB-T, DAB and FM radio signals), assuming that all 4 IOs transmit the same type of waveform (as described in Table 2) in the example scenario shown in Fig. 3 while the target follows the same trajectory. For instance, all 4 transmitters shown in Fig. 3 are now DVB-T IOs and all receivers only process DVB-T signals. Fig. 5 clearly shows that transmitting LFM waveforms by all 4 transmitters substantially outperforms others since the estimated bistatic ranges include less errors if LFM waveforms are transmitted by all IOs. After the LFM waveform, DVB-T

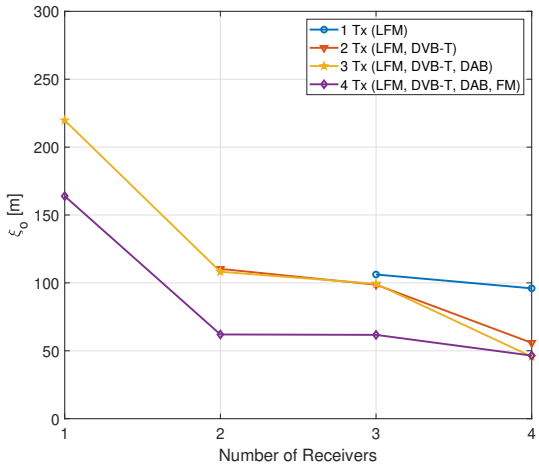

Fig. 7. Average target localization error of the multistatic network with various number of Tx and Rx combinations with average CRLB on range information of the Tx-Rx pairs.

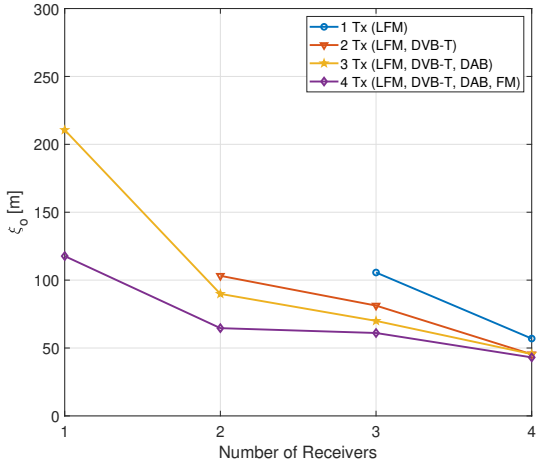

Fig. 8. Average target localization error of the multistatic network with various number of Tx and Rx combinations with exact CRLB on range information of the Tx-Rx pairs for the target position.

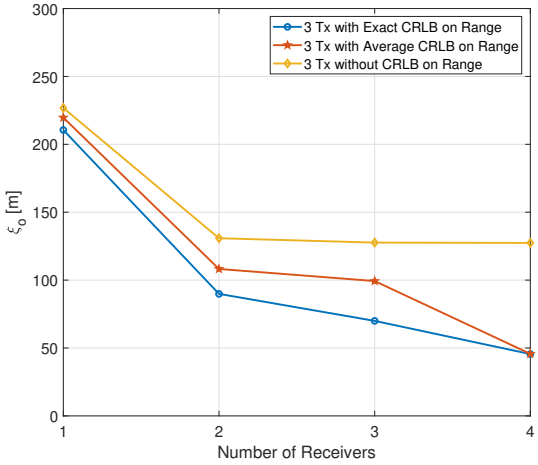

Fig. 9. Average target localization error of the multistatic network with 4 different waveform (Tx) and 3 Rx.

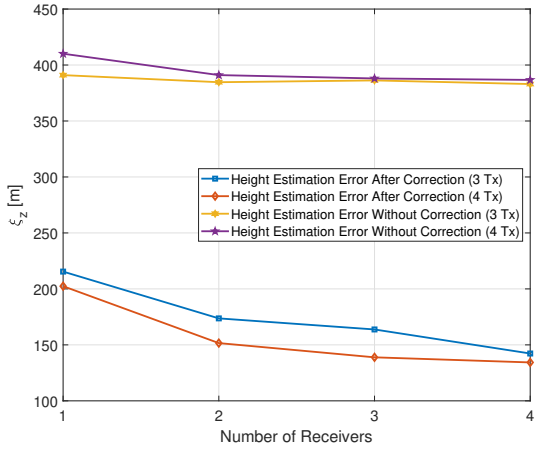

Fig. 10. Average target height estimation error with and without height estimation correction, with 3 Tx and 4 Rx.

signals deliver the second-best estimation accuracy since their bandwidth is wider than DAB and FM radio signals. It is worth noting that not only bandwidth but also the waveform type is also important for range estimation as shown in CRLBs calculations in [15]. The worst localization performance is obtained when all IOs transmit FM radio signals because the FM radio signals have the narrowest bandwidth and also their bandwidth, hence, the range estimation accuracy is highly affected by the content transmitted in the radio station of which signals are utilized for passive sensing. In all of these scenarios, only one waveform type is considered to compare their performance. However, in a real scenario, it is more likely to utilize various waveforms at the same time. Therefore, the next figures present the target localization estimation performance when all IOs transmit different waveforms.

Fig. 6 illustrates the mean absolute error (ξ_o) of location estimation as a function of the number of IOs and receivers when the estimator does not have the knowledge of the CRLBs on the range of pairs. For 3D target localization, at least 3 bistatic range estimations are required, therefore, minimum 3 (i.e., 1 Tx and 3 Rx) and maximum 16 Tx and Rx pairs (i.e., 4 Tx and 4 Rx) are considered for localization. It is obvious that increasing number of transmitters and receivers may not always improve the estimation accuracy since some IOs might have significantly high bistatic range estimation errors. Moreover, the estimation errors will also vary depending on the target location. For instance, having 4 transmitters (LFM, DVB-T, DAB, and FM radio signals) result in a worse location estimation accuracy than the case where only 2 IOs (LFM and DVB-T) are considered. Because, the bistatic range errors introduced by DAB and FM radio signals are significantly higher than LFM and DVB-T signals, therefore including them in location estimation leads to a worse estimation accuracy. However, the estimation accuracy can be improved as shown in Fig. 7, where the location estimator has only the mean CRLBs of all pairs over the entire area of interest. This information can be obtained without knowing the target location. This is also the estimation results of the first stage of the proposed method in Algorithm 1. It is evident that only knowing the average CRLBs on the range of all pairs, the target location estimation accuracy has been substantially improved. In Fig. 7, having 4 IOs transmitting different waveforms provided a better estimation than having 3 or 2 IOs. However, when the number of receivers is 3 or 4, having fewer transmitters might result in a better target location estimation. For further improvement, a more precise knowledge of bistatic CRLBs on the range estimations is necessary.

In the proposed algorithm, the second stage utilizes the initially estimated target location based on the average CRLBs of the pairs and then fetches the corresponding CRLBs to this target location for the second stage. Therefore, it obtains more precise CRLBs on the range and utilizes this information to improve the location estimation. The results of the second stage for this specific multi-waveform multistatic radar network are presented in Fig. 8. This result shows a significant improvement such that including more transmitters and receivers always results in better location estimation accuracy. For instance, FM radio signals cause more estimation errors in bistatic range estimations, knowing CRLBs on this range estimation enables the hybrid multistatic radar network efficiently utilize these signals and improve the target location estimation. Fig. 9 compares the target location estimation accuracy with the three different methods when 3 IOs are utilized for bistatic range and target location estimation. It is clear that the proposed algorithm delivers significantly improved location estimation performance. This shows the importance of modeling the hybrid multistatic radar and calculating CRLBs of all Tx-Rx pairs in advance and utilizing this information in the target location estimation.

The performance of the target height correction stage is presented in Fig. 10, which illustrates the average target height estimation errors of various scenarios. Without any correction, the average error in target height estimation can be as high as 400 meters, but after applying the height correction, the average error becomes about 150 meters. This figure also shows that having a larger number of Tx (IOs) and Rx provides a better target height estimation with the proposed height correction stage.

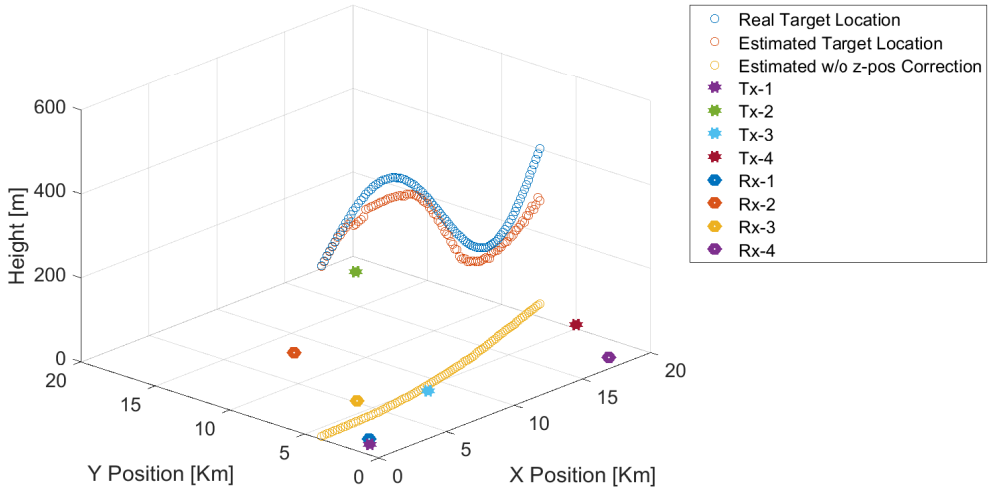

Fig. 11. Target trajectory and estimated target positions using 3 Tx and 4 Rx.

Fig. 11 visualizes an example 3D scenario considered in the simulations, where the location of the transmitter, IOs, and receivers are shown. The target trajectory, estimated target locations with and without target height correction are also shown in this figure. It can be seen that without any height correction, the target height is estimated around the same height as the transmitters and receivers. After height correction, the target height estimation is substantially improved. This figure also shows that the target location estimation accuracy varies depending on the target location since the bistatic range measurements are affected by the bistatic geometries between the Tx-Rx pairs.

The simulation results show that utilizing the precalculated CRLB on the range of each Tx-Rx pair significantly enhances the target localization estimation accuracy since each pair has a different waveform and the geometry of the bistatic pairs with target impacts the range estimation accuracy. Without CRLB on the range information, the performance of localization algorithms tends to be significantly degraded due to significant errors in the bistatic range estimations caused by the bistatic geometry, SINR, and employing various waveforms for sensing at the same time. Accordingly, the proposed algorithm offers significant improvements for the target localization with low computational complexity because it utilizes closed-form equations, and the CRLBs on the range of the entire area is calculated only once and in advance.

V. Conclusion

This study has presented a three-stage algorithm to enhance the target localization accuracy in multi-waveform multi-band multistatic radar networks, where the bistatic ranges estimated by the Tx-Rx pairs are highly dependent on the bistatic geometry of the Tx-Rx pairs, SINR, and the waveforms utilized for radar sensing. The proposed algorithm utilizes the pre-calculated bistatic CRLBs on the range information of all bistatic Tx-Rx pairs while estimating the target location. To achieve this, a 3D model of the multistatic radar network is created and CRLBs on the range estimation of all pairs are calculated for possible target locations in advance. After that, this CRLB information is exploited to improve the target location estimation and rectify the target height estimation in a three-stage algorithm. The proposed algorithm is computationally efficient since it is based on closed-form localization equations. This research demonstrated that the information fusion based on passive bistatic Tx-Rx pairs employing various waveforms can be effectively utilized for the target location estimation in multi-waveform multistatic radar networks.

References

[1] S. Zhang, Y. Zhou, L. Zhang, Q. Zhang, and L. Du, "Target detection for multistatic radar in the presence of deception jamming," *IEEE Sensors Journal*, vol. 21, no. 6, pp. 8130–8141, March 2021.

[2] A. Zaimbashi, "Multistatic passive radar sensing algorithms with calibrated receivers," *IEEE Sensors Journal*, vol. 20, no. 14, pp. 7878–7885, July 2020.

[3] J. S. Patel, F. Fioranelli, M. Ritchie, and H. D. Griffiths, "Fusion of deep representations in multistatic radar networks to counteract the presence of synthetic jamming," *IEEE Sensors Journal*, vol. 19, no. 15, pp. 6362–6370, Aug 2019.

[4] H. D. Griffiths and C. J. Baker, *An introduction to passive radar*. Artech House, 2017.

[5] H. Kuschel, J. Heckenbach, and J. Schell, "Deployable multiband passive/active radar for air defense (DMPAR)," *IEEE Aerospace and Electronic Systems Magazine*, vol. 28, no. 9, pp. 37–45, Sep. 2013.

[6] H. Griffiths and C. Baker, "Passive coherent location radar systems. part 1: Performance prediction," *IEE Proceedings-Radar, Sonar and Navigation*, vol. 152, no. 3, pp. 153–159, 2005.

[7] D. Dhulashia, M. Temiz, and M. A. Ritchie, "Jamming effects on hybrid multistatic radar network range and velocity estimation errors," *IEEE Access*, vol. 10, pp. 27 736–27 749, 2022.

[8] V. Winkler, D. Fränken, C. Erhart, O. Zeeb, and S. Lutz, "Multistatic multiband passive radar - architecture and sensor cluster results," in *2019 IEEE Radar Conference (RadarConf)*, April 2019, pp. 1–6.

[9] M. Edrich, "Design and performance evaluation of a mature FM/DAB/DVB-T multi-illuminator passive radar system," *IET Radar, Sonar & Navigation*, vol. 8, pp. 114–122(8), February 2014.

[10] D. Gould, "Developments to a multiband passive radar demonstrator system," *IET Conference Proceedings*, pp. 188–188(1), January 2007.

[11] M. Edrich, S. Lutz, and F. Hoffmann, "Passive radar at Hensoldt: A review to the last decade," in *2019 20th International Radar Symposium (IRS)*, June 2019, pp. 1–10.

[12] H. Kuschel, M. Ummenhofer, P. Lombardo, F. Colone, and C. Bongioanni, "Passive radar components of ARGUS 3D," *IEEE Aerospace and Electronic Systems Magazine*, vol. 29, no. 3, pp. 15–25, March 2014.
[13] Q. He and R. S. Blum, "The significant gains from optimally processed multiple signals of opportunity and multiple receive stations in passive radar," *IEEE Signal Processing Letters*, vol. 21, no. 2, pp. 180–184, Feb 2014.
[14] V. Anastasio, "Cramér-Rao lower bound with $P_d < 1$ for target localisation accuracy in multistatic passive radar," *IET Radar, Sonar & Navigation*, vol. 8, pp. 767–775(8), August 2014.
[15] M. Temiz, M. Ritchie, and H. Griffiths, "Waveform selection for multi-band multistatic radar networks," *TechRxiv*, vol. preprint, 3 2022. [Online]. Available: https://www.techrxiv.org
[16] S. Choi, D. Crouse, P. Willett, and S. Zhou, "Multistatic target tracking for passive radar in a DAB/DVB network: initiation," *IEEE Transactions on Aerospace and Electronic Systems*, vol. 51, no. 3, pp. 2460–2469, July 2015.
[17] M. Malanowski and K. Kulpa, "Two methods for target localization in multistatic passive radar," *IEEE Transactions on Aerospace and Electronic Systems*, vol. 48, no. 1, pp. 572–580, Jan 2012.
[18] M. Dianat, M. R. Taban, J. Dianat, and V. Sedighi, "Target localization using least squares estimation for MIMO radars with widely separated antennas," *IEEE Transactions on Aerospace and Electronic Systems*, vol. 49, no. 4, pp. 2730–2741, OCTOBER 2013.
[19] P. Addesso, S. Marano, and V. Matta, "Estimation of target location via likelihood approximation in sensor networks," *IEEE Transactions on Signal Processing*, vol. 58, no. 3, pp. 1358–1368, March 2010.
[20] H. Godrich, A. M. Haimovich, and R. S. Blum, "Target localization accuracy gain in MIMO radar-based systems," *IEEE Transactions on Information Theory*, vol. 56, no. 6, pp. 2783–2803, June 2010.
[21] Y. Zhao, Y. Zhao, and C. Zhao, "A novel algebraic solution for moving target localization in multi-transmitter multi-receiver passive radar," *Signal Process.*, vol. 143, no. C, p. 303–310, feb 2018. [Online]. Available: https://doi.org/10.1016/j.sigpro.2017.09.014
[22] L. Rui and K. C. Ho, "Elliptic localization: Performance study and optimum receiver placement," *IEEE Transactions on Signal Processing*, vol. 62, no. 18, pp. 4673–4688, Sep. 2014.
[23] A. Noroozi, M. A. Sebt, S. M. Hosseini, R. Amiri, and M. M. Nayebi, "Closed-form solution for elliptic localization in distributed MIMO radar systems with minimum number of sensors," *IEEE Transactions on Aerospace and Electronic Systems*, vol. 56, no. 4, pp. 3123–3133, Aug 2020.
[24] A. Noroozi, R. Amiri, M. M. Nayebi, and A. Farina, "Efficient closed-form solution for moving target localization in MIMO radars with minimum number of antennas," *IEEE Transactions on Signal Processing*, vol. 68, pp. 2545–2557, 2020.
[25] A. Noroozi and M. A. Sebt, "Target localization from bistatic range measurements in multi-transmitter multi-receiver passive radar," *IEEE Signal Processing Letters*, vol. 22, no. 12, pp. 2445–2449, Dec 2015.
[26] R. Amiri, F. Behnia, and H. Zamani, "Asymptotically efficient target localization from bistatic range measurements in distributed MIMO radars," *IEEE Signal Processing Letters*, vol. 24, no. 3, pp. 299–303, March 2017.
[27] A. Noroozi, A. H. Oveis, and M. A. Sebt, "Iterative target localization in distributed MIMO radar from bistatic range measurements," *IEEE Signal Processing Letters*, vol. 24, no. 11, pp. 1709–1713, Nov 2017.
[28] R. Amiri, F. Behnia, and M. A. M. Sadr, "Exact solution for elliptic localization in distributed MIMO radar systems," *IEEE Transactions on Vehicular Technology*, vol. 67, no. 2, pp. 1075–1086, Feb 2018.
[29] B. K. Chalise, Y. D. Zhang, M. G. Amin, and B. Himed, "Target localization in a multi-static passive radar system through convex optimization," *Signal Processing*, vol. 102, pp. 207–215, 2014.
[30] F. Zhang, Y. Sun, J. Zou, D. Zhang, and Q. Wan, "Closed-form localization method for moving target in passive multistatic radar network," *IEEE Sensors Journal*, vol. 20, no. 2, pp. 980–990, Jan 2020.
[31] M. S. Greco, P. Stinco, F. Gini, and A. Farina, "Cramer-rao bounds and selection of bistatic channels for multistatic radar systems," *IEEE Transactions on Aerospace and Electronic Systems*, vol. 47, no. 4, pp. 2934–2948, October 2011.
[32] G. Cui, J. Liu, H. Li, and B. Himed, "Signal detection with noisy reference for passive sensing," *Signal Processing*, vol. 108, pp. 389–399, 2015.
[33] M. A. Alslaimy, R. J. Burkholder, and G. E. Smith, "Measurements accuracy evaluation for ATSC signal based passive radar systems," *IEEE Transactions on Aerospace and Electronic Systems*, pp. 1–1, 2021.
[34] F. Colone, D. W. O'Hagan, P. Lombardo, and C. J. Baker, "A multistage processing algorithm for disturbance removal and target detection in passive bistatic radar," *IEEE Transactions on Aerospace and Electronic Systems*, vol. 45, no. 2, pp. 698–722, April 2009.
[35] A. Dogandzic and A. Nehorai, "Cramer-rao bounds for estimating range, velocity, and direction with an active array," *IEEE Transactions on Signal Processing*, vol. 49, no. 6, pp. 1122–1137, June 2001.
[36] A. Filip and D. Shutin, "Cramér–Rao bounds for L-band digital aeronautical communication system type 1 based passive multiple-input multiple-output radar," *IET Radar, Sonar & Navigation*, vol. 10, no. 2, pp. 348–358, 2016.
[37] M. Greco, P. Stinco, F. Gini, A. Farina, and M. Rangaswamy, "Cramér-Rao bounds and Tx-Rx selection in a multistatic radar scenario," in *2010 IEEE Radar Conference*, May 2010, pp. 1371–1376.

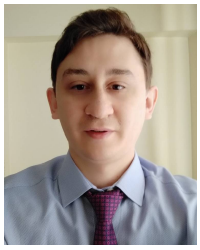

Murat Temiz (S'19-M'20) received the M.Sc. degree in Electrical and Electronics Engineering from TOBB University of Economics and Technology, in Ankara, Turkey. He received the Ph.D. degree in Electrical and Electronic Engineering at the University of Manchester, U.K., in 2020. His current research interests are massive MIMO communication systems, dual-function radar and communication systems, multistatic and passive radar networks and applications of machine learning techniques in communication and radar systems.

Hugh Griffiths (Fellow, IEEE) received the M.A. degree in physics from Oxford University, Oxford, U.K., in l975, and the Ph.D. and D.Sc. (Eng.) degrees in electronic engineering from University College London, London, U.K., in 1986 and 2000, respectively. He holds the THALES/Royal Academy of Engineering Chair of RF sensors with the Department of Electronic and Electrical Engineering, University College London.

He has authored or coauthored more than 500 papers and technical articles in the fields of radar, antennas, and sonar. His research interests include radar and sonar systems, signal processing (particularly synthetic aperture radar and bistatic radar), and antenna measurement techniques. He was appointed as the Officer of the Order of the British Empire in the 2019 Queen's New Year's Honours List. He became a fellow of the Royal Academy of Engineering in 1997. He is a fellow of the IET and the IEEE.

Matthew A. Ritchie (M'10-SM'20) Dr. Matthew Ritchie received the M.Sci. degree in physics from The University of Nottingham, in 2008. Following this he completed the Eng.D. degree at University College London (UCL), London, U.K., in association with Thales U.K., in 2013. He then worked as a postdoctoral research associate focusing on machine learning applied to multistatic radar for micro-Doppler classification. In 2017 Dr. Ritchie took a Senior Radar Scientist position at the Defence Science and Technology Laboratories (Dstl). He is now an associate professor at UCL within the Radar Sensing group and focused on areas including multistatic radar, passive radar, micro-Doppler and multi-role RF sensor hardware.

Currently he serves as the Chair of the IEEE Aerospace and System Society (AESS) for the United Kingdom Ireland, is a Subject Editor-in-Chief for the IET Electronics Letters journal and a Senior Member of the IEEE and the head of the UK EMSIG Society. He was awarded the 2017 IET RSN best paper award as well as the Bob Hill Award at the 2015 IEEE International Radar Conference.